Doppler Characteristics of Sea Clutter at K-band and W-band: Results from the St Andrews and Coniston Water Trials

Samiur Rahman
SUPA School of Physics & Astronomy
University of St Andrews
St Andrews, Scotland
sr206@st-andrews.ac.uk
https://orcid.org/0000-0002-5477-4218

Aleksanteri B Vattulainen
SUPA School of Physics & Astronomy
University of St Andrews
St Andrews, Scotland
av41@st-andrews.ac.uk
https://orcid.org/0000-0003-1898-600X

Duncan A Robertson
SUPA School of Physics & Astronomy
University of St Andrews
St Andrews, Scotland
dar@st-andrews.ac.uk
https://orcid.org/0000-0002-4042-2772

***Abstract*—This study reports on the experimental results from two field trials conducted by the University of St Andrews, focusing exclusively here on Doppler data. The first trial was at the Bruce Embankment in St Andrews, UK (winter 2020) and the second one was at Coniston Water in the Lake District, UK (autumn 2022). A 24 GHz K-band radar and a 94 GHz W-band radar were used in both trials to collect sea clutter data for phenomenology studies. As very few sea clutter data and analysis of these are available in the literature at these high frequencies, the results are expected to be of general interest within this field of study. The data collection at both trials was done for low grazing angles in the littoral zone. The datasets are quite varied in terms of wave direction, polarization and wind speed. The Doppler signatures and corresponding statistical parameters for these various conditions are reported here. The spectral analysis of different wave types (burst, whitecap, rough surface scattering) along with the combined spectra are also discussed. It is anticipated that these empirical results will be the precursor for improving upon the frequency ranges of existing sea clutter Doppler models.**

Keywords— Sea clutter, sea-spikes, breaking waves, Doppler, millimeter wave, FMCW, K-band, W-band

I. INTRODUCTION

The study of radar sea clutter returns is of great interest for maritime navigation. Doppler signatures can be used for discriminating targets from clutter returns and thorough understanding of the Doppler characteristics enables more reliable classification algorithm development. As K-band and W-band radar hardware technology have become more advanced and affordable due to the automotive industry, exploring the use of sensors for autonomous marine vessels at these frequencies has also generated interest. Radars at these frequencies benefit from better Doppler sensitivity, where they could potentially become key sensors by using Doppler as one of the feature spaces.

Comprehensive analysis of sea clutter Doppler properties is required for such sensor design in marine autonomy. Currently, the open literature has no thorough analysis of sea clutter Doppler beyond X-band. Experimental results at K-band and W-band are also quite scarce. In [1], [2], extensive analysis of medium grazing angle Doppler spectra characterization and model assessment has been done using X-band airborne radar data. The derivation of the models is based on the statistical properties of the radar data Doppler spectra. Improved parametric modeling of the Doppler spectra was demonstrated in [3], which incorporates radar resolved area and integration time. This work was also based on the X-band radar dataset. In [4], a comprehensive report of the empirical observations of the Doppler spectrum at low and high grazing angles is presented, along with various mathematical models based on the measured Doppler spectra. Again, the empirical results are mainly at X-band. It also incorporates a model for Ku-band, which was developed by using low grazing angle 15.75 GHz experimental Doppler data [5]. Detailed Doppler analysis of medium-to-low grazing angles is also presented in [6], which uses the X-band CSIR Fynmeet radar database [7]

The work presented here is part of a project which explores radar sea clutter signatures ranging from 24 GHz to 300 GHz, to support the development of sensors for future autonomous marine vessels. In this particular study, the motivation is to illustrate the nature of the Doppler properties of the sea surface at 24 GHz and 94 GHz. These two frequencies are strong candidates for future sensors given the performance, compactness, and price of the underlying hardware technology. The rest of this paper details two field trials, spectral properties obtained from the measured data at low grazing angles (1°-3°) and finally the method of calculating Doppler velocity from range-time intensity data.

II. SUMMARY OF FIELD TRIALS

The first field trial was held at the Bruce Embankment, St Andrews, UK on the 15 December 2020. The trial location coordinates are 56°20′41″ N 2°48′06″ W. As seen in Fig. 1(b)-(c), the two radars collected data of waves receding from the radar while pointing at the shore and waves approaching the radar when they were pointing towards the open sea. The wind speed was ~13 km/h from the South, the air temperature was 8 °C and the Douglas sea state was 0-1 for the duration of the data collection. The second trial was conducted at Coniston Water, Lake District, UK (54°20'50.67" N 3°4'48.62" W). This campaign lasted for three days (30 August 2022-1 September2022). As seen in Fig. 1(d), the radars pointed across the lake for data collection, but changed staring direction at various points. Fig. 1(b) shows three radars, as a G-band 207 GHz radar [8] was also used in this trial, results from which are not included in this paper. As the radars were places on the shore, all the clutter datasets comprised of approaching waves. There was no great variation in sea state conditions.

UK Engineering and Physical Sciences Research Council under grant EP/S032851/1

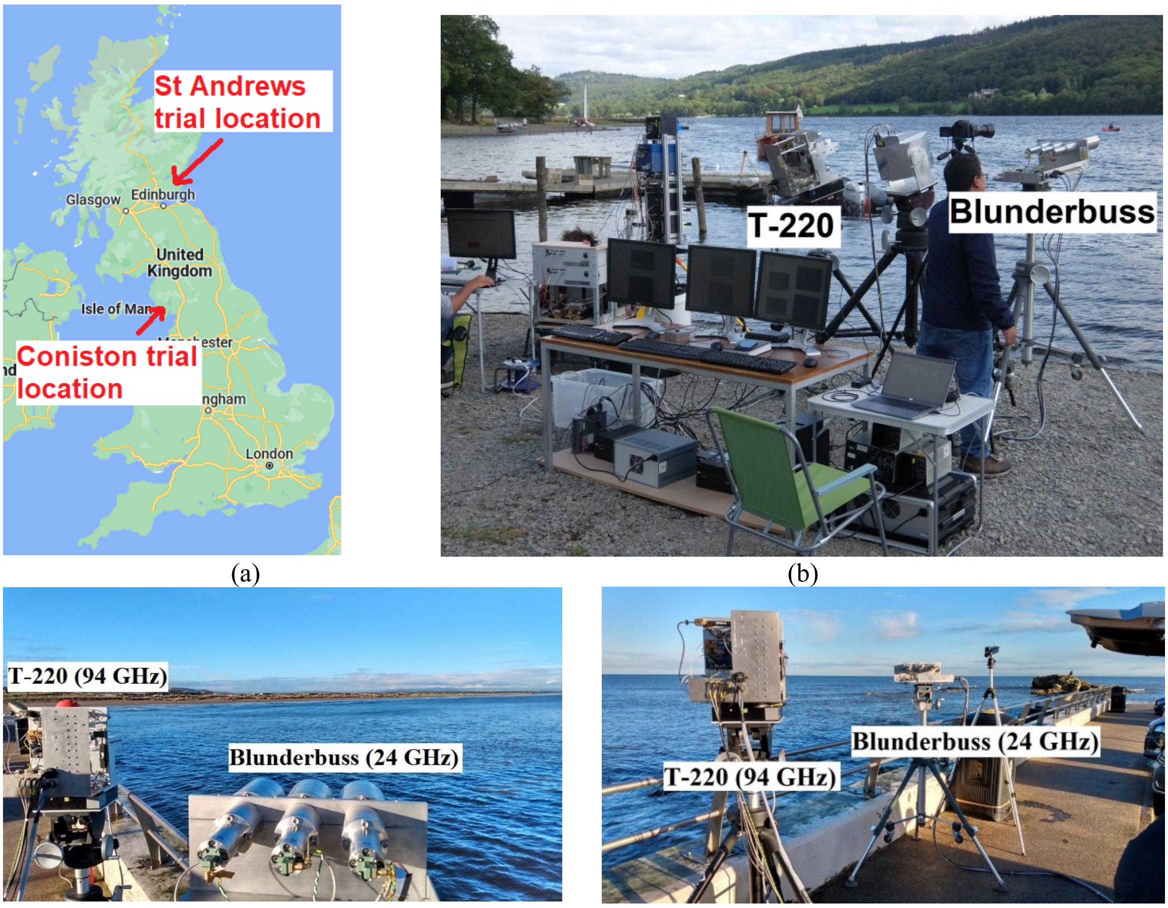

Figure 1. (a) Location of the field trials; (b) field trial setup at Coniston Water trial; (c) radars pointing towards the beach at St Andrews trial; (d) radars pointing towards the open sea at St Andrews trial.

Mild to moderate wind was observed during the whole trial, with intermittent gusts. The wind speed was below 10 km/h for most of the time and reached 15-20 km/h during gusts. Maximum wind speeds recorded each day were 21-22 km/h. The wave conditions here were also sea state 0-1. Although the Coniston data are of a lake surface, for brevity the term 'sea clutter' is used here to define all the datasets, as small to medium sized commercial boats would often deal with clutter returns from both sea and lake/freshwater surfaces.

The two coherent Frequency Modulated Continuous Wave (FMCW) radars used in the trials were designed and built by the Millimetre Wave Group at the University of St Andrews. The 24 GHz radar (Blunderbuss) is an Analog Devices evaluation board based radar system [9]. The radar operates coherently by using the internal 100 MHz reference clock of the board as the input to the radar frequency chain and by triggering the ADC externally from the chirp end signal from the board. The circularly symmetric horn antennas used for the radar were also designed and built in-house. The 94 GHz radar (T-220) is a Direct Digital Synthesizer (DDS) based very low phase noise system, with narrow fan beam antenna beam patterns [10]. As seen in Fig. 1(d), each radar has a dedicated PC for control and data capture.

Blunderbuss is linearly polarized with one transmit horn and two receive horns for simultaneous reception in co- and cross-polarization. By rotating the transmit horn between runs data was collected in Vertical-Vertical (VV) and Vertical-Horizontal (VH) or Horizontal-Horizontal (HH) and Horizontal-Vertical (HV). Meanwhile, the T-220 radar has a fixed circular polarization (CP), with odd bounce, transmitting right CP and receives left CP. The radar specifications are in Table I. In the first trial at St Andrews, 24 GHz data were collected only for VV and VH. At Coniston the polarization was changed multiple times throughout the three days for Blunderbuss. The other difference is that the datasets from the first trial are not

TABLE I: 24 AND 94 GHZ RADAR SPECIFICATIONS

Parameter	*Blunderbuss*	*T-220*
Center Frequency	24 GHz	94 GHz
Modulation	FMCW	FMCW
Antenna beamwidth (one-way)	11.2° az., 11.2° el.	0.92° az., 3° el.
Antenna gain	24.5 dBi	40.5 dBi
Polarization	Linear (HH, VVl)	Circular (odd bounce)
Tx power	+25 dBm	+18 dBm
Bandwidth / range resolution	250 MHz / 60 cm	750 MHz / 20 cm
Chirp Repetition Interval (CRI)	357.44 µs	122.34 µs
Maximum unambiguous velocity	± 8.74 ms^{-1}	± 6.54 ms^{-1}
Instrumented range	307.2 m	204.8 m

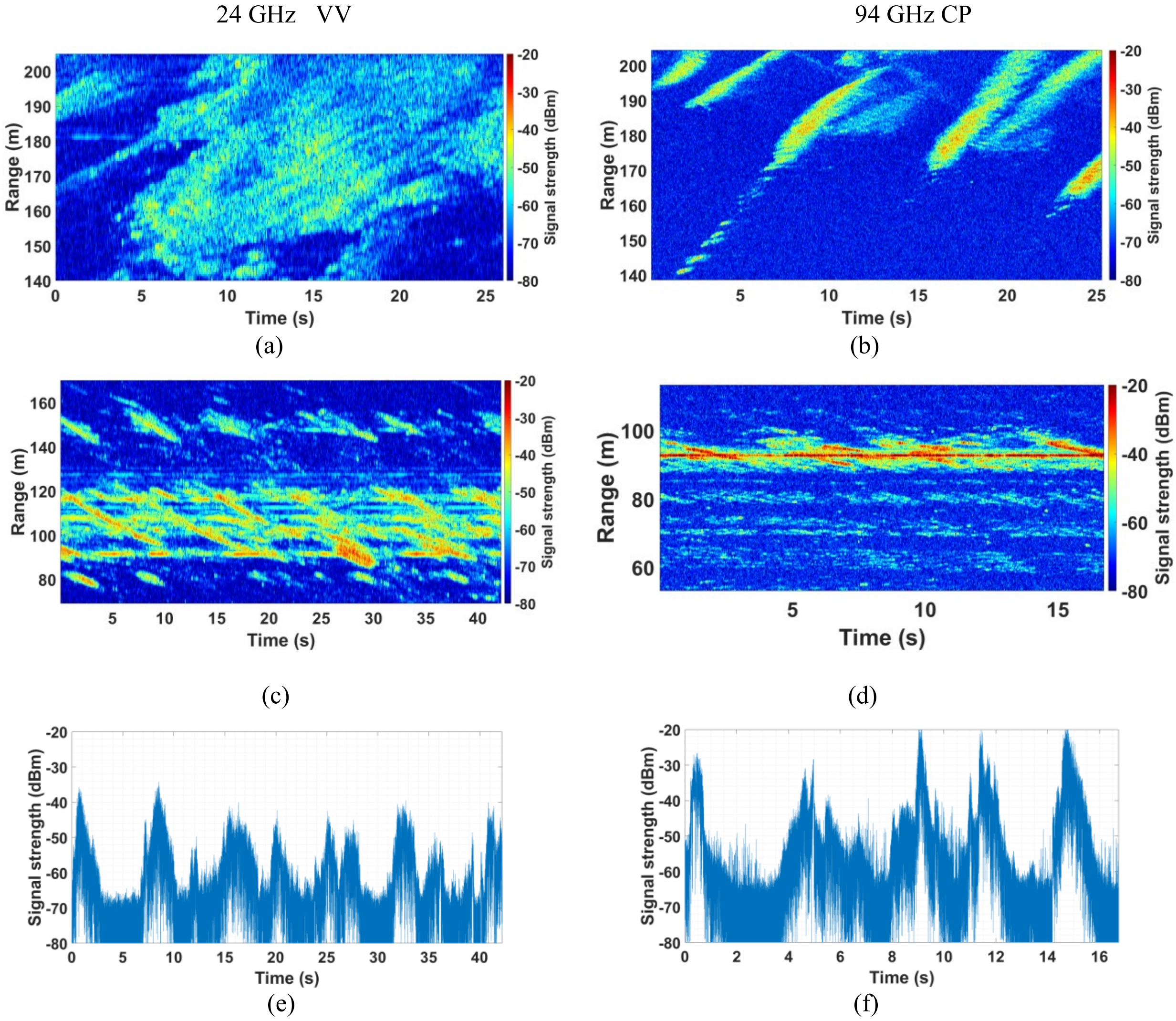

Fig. 2. (a),(c),(e) 24 GHz VV range-time-intensity plots and range slice time history; (b),(d),(f) 94 GHz CP range-time-intensity plots and range slice time history from the St Andrews trial.

simultaneous for both frequencies but offset by a few seconds because the data files were being saved separately on the respective PCs manually. For the second trial a trigger switch box was made to synchronize the data saving. Hence, the Coniston trial data for different radars are time aligned.

III. Doppler Spectrum Results

For Doppler analysis, time history plots of a range slice are observed to select different wave components. The definitions of sea-spikes are somewhat varied in the literature, but here generally follows the descriptions in [6].

Fig. 2 shows range-time-intensity plots from the St Andrews trial. In general, it was observed that the 24 GHz returns are comparatively more distributed (less spiky) than the 94 GHz. This may be due to the combination of Blunderbuss having both a wider beamwidth and coarser range resolution. The horizontal lines in Fig. 2(c)-(d) are returns from a rock protruding above the water's surface. Fig. 2 (e)-(f) shows example time histories of the signal returns for a given range slice. From these, different wave types are selected for Doppler spectra parameter calculations.

Fig. 3 shows the time history plots of different wave types with their corresponding Doppler spectrum. The peak Doppler frequency, Full Width Half Maximum (FWHM), and second, third and fourth central moment (standard deviation, skewness and kurtosis respectively) values are shown for each spectrum. The largest FWHM values are observed for 94 GHz approaching breaking waves and whitecaps. In the case of 24 GHz, the largest FWHM is also for breaking waves. The largest standard deviation values are likewise found for breaking waves. The highest kurtosis value is seen for burst scattering for both frequencies, which again is perhaps not unexpected. The wind speed was fairly mild and consistent for all the datasets (~13 km/h with wave direction mostly towards the shore).

The Coniston trial Doppler results are shown in Fig. 4. Doppler sensitivity across the instrumented range was higher as the wave direction was more radially along the radar beam compared to the St Andrews data. The 94 GHz datasets showed very strong clutter sensitivity. It appears to be more sensitive to clutter than the 24 GHz from the overall inspection, but this is not entirely conclusive. This may be due to the fact mentioned earlier regarding the antenna beamwidth and resolution. Also, the T-220 hardware has better sensitivity and phase noise performance than Blunderbuss. The phase noise effect can be seen in the

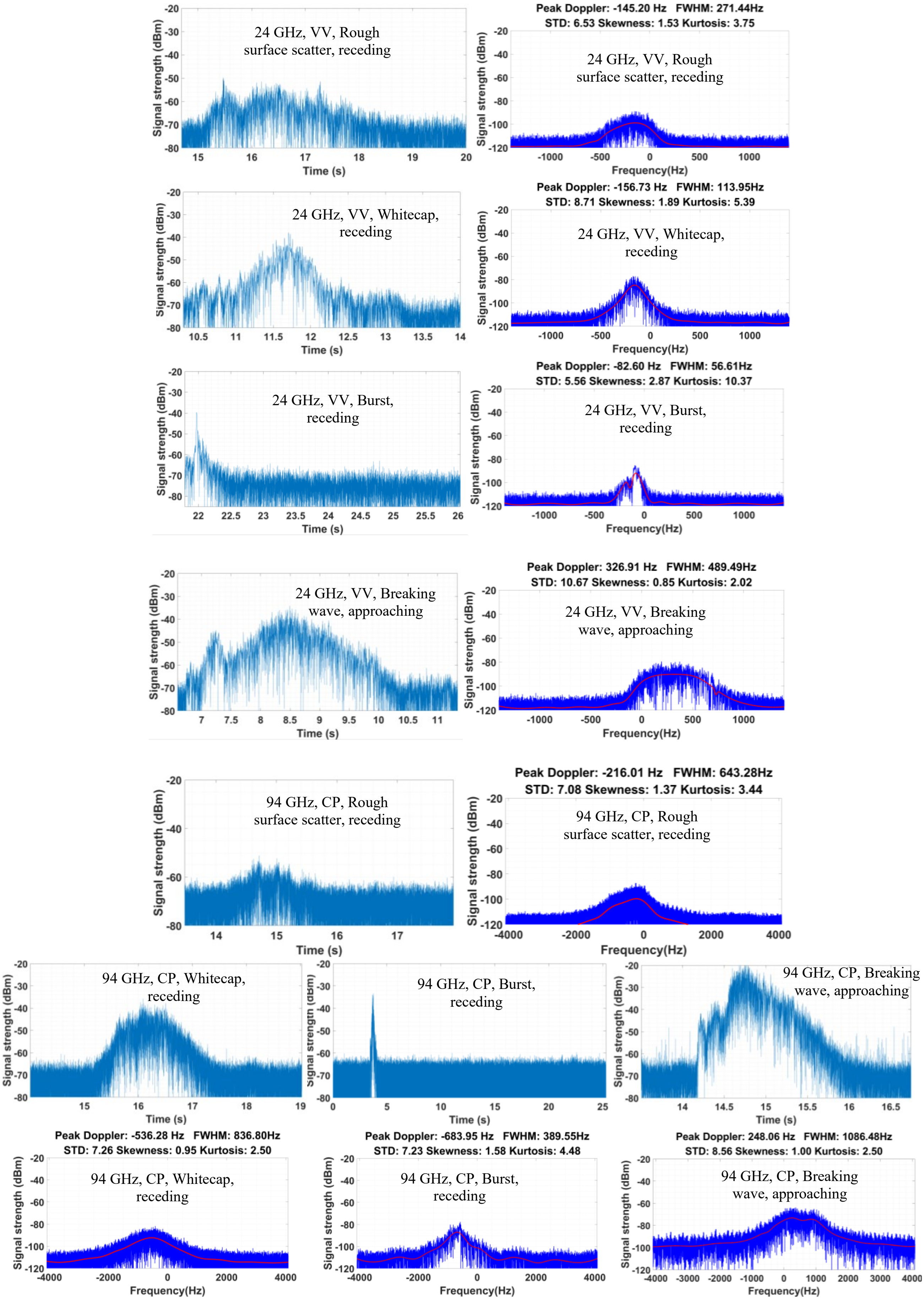

Fig. 3. Time history of range slices of waves and their corresponding Doppler spectra from the St Andrews trial data.

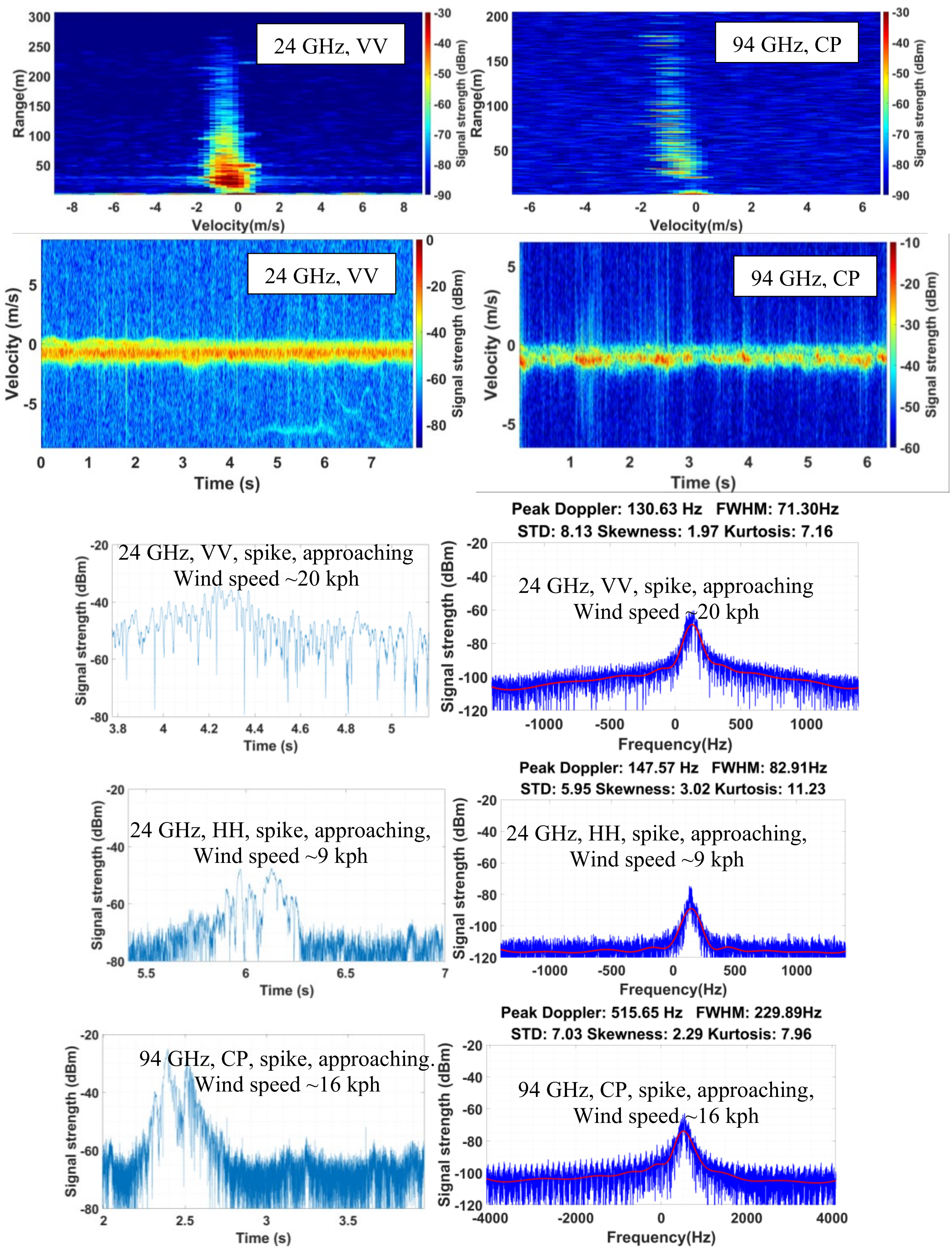

Fig. 4. Doppler results from the Coniston trial, simultaneous range-Doppler and spectrogram plots in the top two rows at 24 and 94 GHz showing the clutter sensitivity at both frequencies, then in the bottom three rows showing the time history of range slices of waves and their corresponding Doppler. spectra.

Fig. 4 24 GHz time history VV plot showing the raised noise floor level due to high wind generating strong returns from close range. The reflected phase noise from bright returns slightly increases the corresponding Doppler noise floor around the peak Doppler as well. No discernible difference between the 24 GHz HH and VV Doppler spectra has yet been found. The kurtosis values are in general higher in the Coniston data than the St Andrews data. This may be due to the greater 'spikiness' of the waves in the Coniston datasets. No breaking wave/whitecap scattering was observed, perhaps due to the low to moderate wind speed and shorter fetch over the lake meaning waves had less energy than the sea waves when breaking onto the shore.

A. Range-time Doppler results

Calculation of the instantaneous velocity was done to produce range-time Doppler plots. These plots are convenient for visualizing various velocity components and their progression within the scene. The following methodology was used to generate the plots. Initially,

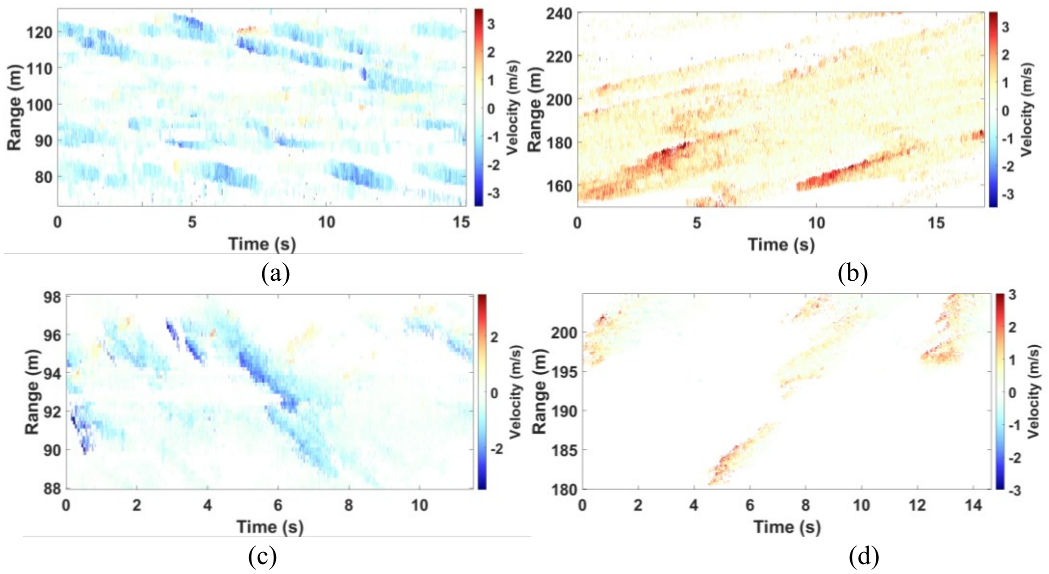

Fig. 5. (a)-(b) 24 GHz range-time Doppler plots in VV from the St Andrews trial; (c)-(d) 94 GHz range-time Doppler plots in CP from the St Andrews trial.

spectrograms are produced for every range slice in time. Then the center of mass for each Doppler slice of the spectrogram is calculated. The corresponding Doppler velocity is then selected as the pixel value. The process is then repeated for all the range bins of interest. Constant False Alarm Rate (CFAR) thresholding is done as pre-processing to eliminate points corresponding to noise, spray or low level rough surface scatter. An expected probability of false alarm of $P_{fa} = 10^{-4}$ was used during cell averaging CFAR detection, where the number of training and guard cells were 200 and 10, respectively. This makes the plots less noisy and easier to visualize. Fig. 5 shows example range-time Doppler plots produced from the St Andrews trial data. The blue shift of the incoming waves and the red shift of the receding breaking waves can be observed along with the velocity component changes within a wave progression. The waves here show banding patterns, which correspond to the crest and trough. This means it is possible to calculate the orbital velocity and subsequently the phase velocity and the sea-spike wavelength [11]. The detailed analysis will be reported in a separate publication.

IV. Conclusion

Early results of the processed sea clutter Doppler data from two different field trials in the UK have been reported in this paper. Both trials were very successful in collecting large amounts of low grazing angle, low sea-state data, at 24 GHz and 94 GHz, which are not readily available. Various Doppler properties (central moments and FWHM) have been calculated and stated for different kinds of waves at different polarizations and wind conditions. The results here should be useful to adapt the existing Doppler models to these higher frequency bands. More detailed analysis of the empirical observations encompassing more of the collected dataset will be reported in a future publication. Range-time Doppler analysis of the trial data has also been performed and briefly illustrated here, which is also ongoing work that will be beneficial for more in depth clutter analysis.

Acknowledgment

The authors thank the staff at the Raymond Priestley Centre for their help over the duration of the trial.

References

[1] S. Watts, L. Rosenberg, S. Bocquet, and M. Ritchie, “Doppler spectra of medium grazing angle sea clutter; part 1: characterisation,” *IET Radar, Sonar & Navigation*, vol. 10, no. 1, pp. 24–31, Jan. 2016, doi: 10.1049/iet-rsn.2015.0148.

[2] S. Watts, L. Rosenberg, S. Bocquet, and M. Ritchie, “Doppler spectra of medium grazing angle sea clutter; part 2: model assessment and simulation,” *IET Radar, Sonar & Navigation*, vol. 10, no. 1, pp. 32–42, Jan. 2016, doi: 10.1049/iet-rsn.2015.0149.

[3] L. Rosenberg, “Parametric Modeling of Sea Clutter Doppler Spectra,” *IEEE Transactions on Geoscience and Remote Sensing*, vol. 60, 2022, doi: 10.1109/TGRS.2021.3107950.

[4] A. Raynal and A. Doerry, “Doppler characteristics of sea clutter.,” Albuquerque, NM, and Livermore, CA (United States), Jun. 2010. doi: 10.2172/992329.

[5] D. Walker, “Experimentally motivated model for low grazing angle radar Doppler spectra of the sea surface,” *IEE Proceedings - Radar, Sonar and Navigation*, vol. 147, no. 3, p. 114, 2000, doi: 10.1049/ip-rsn:20000386.

[6] K. Ward, R. Tough, and S. Watts, *Sea Clutter: Scattering, the K Distribution and Radar Performance*. Institution of Engineering and Technology, 2013. doi: 10.1049/PBRA025E.

[7] P. L. Herselman, C. J. Baker, and H. J. De Wind, “An Analysis of X-Band Calibrated Sea Clutter and Small Boat Reflectivity at Medium-to-Low Grazing Angles,” *International Journal of Navigation and Observation*, vol. 347518, p. 14, 2008, doi: 10.1155/2008/347518.

[8] A. B. Vattulainen, S. Rahman, and D. A. Robertson, “G-band FMCW Doppler radar for sea clutter and target characterization,” in *Proc. SPIE 10633, Radar Sensor Technology XXII*, 2018, pp. 1–9, doi: 10.1117/12.2618497.

[9] S. Rahman and D. A. Robertson, “Coherent 24 GHz FMCW radar system for micro-Doppler studies,” in *Proc. SPIE 12108, Radar Sensor Technology XXVI*, 2022, 907719, doi: 10.1117/12.2304368.

[10] D. A. Robertson, G. M. Brooker, and P. D. L. Beasley, “Very low-phase noise, coherent 94GHz radar for micro-Doppler and vibrometry studies,” ,” in *Proc. SPIE 9077, Radar Sensor Technology XVIII*, p. 292-300, 2022, doi: 10.1117/12.2053015.

[11] V. G. Gutnik, G. P. Kulemin, and L. I. Sharapov, “Spike statistics features of the radar sea clutter in the millimeter wave band at extremely small grazing angles,” in *4th Int. Kharkov Symp. “Physics and Eng. of Millimeter and Sub-Millimeter Waves”,* Institute of Electrical and Electronics Engineers Inc., pp. 426–428, 2001, doi: 10.1109/MSMW.2001.946876.